LETTERS
PUBLISHED ONLINE: 7 OCTOBER 2012 | DOI: 10.1038/NMAT3430
nature materials

# A magnetic switch for the control of cell death signalling in *in vitro* and *in vivo* systems

Mi Hyeon Cho[1†], Eun Jung Lee[1,2†], Mina Son[2†], Jae-Hyun Lee[1], Dongwon Yoo[1], Ji-wook Kim[1], Seung Woo Park[3], Jeon-Soo Shin[2,4*] and Jinwoo Cheon[1,2*]

**The regulation of cellular activities in a controlled manner is one of the most challenging issues in fields ranging from cell biology to biomedicine[1,2]. Nanoparticles have the potential of becoming useful tools for controlling cell signalling pathways in a space and time selective fashion[3,4]. Here, we have developed magnetic nanoparticles that turn on apoptosis cell signalling by using a magnetic field in a remote and non-invasive manner. The magnetic switch consists of zinc-doped iron oxide magnetic nanoparticles[5] ($Zn_{0.4}Fe_{2.6}O_4$), conjugated with a targeting antibody for death receptor 4 (DR4) of DLD-1 colon cancer cells. The magnetic switch, in its On mode when a magnetic field is applied to aggregate magnetic nanoparticle-bound DR4s, promotes apoptosis signalling pathways. We have also demonstrated that the magnetic switch is operable at the micrometre scale and that it can be applied in an *in vivo* system where apoptotic morphological changes of zebrafish are successfully induced.**

Cell signalling is an important process in biological systems for exchanging information through networks of various signal molecules to control cellular activities, such as differentiation, growth, metabolism and death[6]. Owing to their newly developed high precision and accuracy, physical stimuli using optical, electrical and magnetic methods have been devised to regulate cell signalling[1–4]. Among these, magnetic techniques are uniquely advantageous because magnetic fields can penetrate deeply with negligible attenuation into biological tissues[7,8]. Consequently, it has distinctive benefits for *in vivo* applications. Moreover, when coupled with magnetic nanoparticles, magnetic fields can be transformed into other forms of energy, such as heat and mechanical force[9–16]. The magnetic heat induction has been used for gating of the thermosensitive ion channel[9] as well as for hyperthermia therapy[10]. Although relatively large mechanical force (in the piconewton range) has been used in *in vitro* and *in vivo* systems for direct stretching of ion channels and cytoskeletal stimulation[11–13], two recent *in vitro* studies have revealed that the induction of calcium influx[15] and tubulogenesis[16] using receptor clustering is also possible by using nanoparticles. Magnetic nanoparticles can exert a gentle force (in the femtonewton range) on membrane receptors to induce their clustering without disturbing the rheological and cytoskeletal properties. Furthermore, the nanoscale dimensions of nanoparticles conjugated with targeting molecules make them beneficial for probing cellular sensory structures and functions at the molecular level and for inducing specific cellular activation processes[7,8]. Nonetheless, the nanoscale magnetic switching technique for receptor clustering is still at too early a stage of development to guarantee that it will be generally applicable to the control of cell signalling in other biologically important systems. In addition, it is not known whether it will be effective in *in vivo* systems.

Apoptosis, programmed cell death, is known to be a major factor in maintaining homeostasis and removing undesired cells[17–19]. Recently, an extrinsic apoptosis signalling pathway that is initiated by death receptors has emerged as one of the main targets for cancer therapy[20–22]. Extrinsic apoptosis signalling is usually activated by clustering of death receptors through docking of biochemical ligands, such as the TNF-related apoptosis inducing ligand (TRAIL) that is a potent inducer of apoptosis[23,24]. However, direct use of such ligands in clinical applications is limited by the short plasma half-life and the ease of degradation[25,26].

In the study described below, we have developed a magnetic switch for apoptosis signalling, and demonstrate its *in vivo* feasibility through the receptor clustering process (Fig. 1). The magnetic switch for cell signalling consists of DR4 monoclonal antibody conjugated to magnetic nanoparticles (Ab–MNPs). DR4s are highly expressed on tumour cells[20–27] and magnetic nanoparticles are designed to bind DR4s through a specific monoclonal antibody interaction. Zinc-doped iron oxide magnetic nanoparticles ($Zn_{0.4}Fe_{2.6}O_4$ MNPs, 15 nm) are chosen (Fig. 2a) owing to their high saturation magnetization value (161 e.m.u. $g^{-1}$), which is essential for effective utilization of magnetic force[5] (Supplementary Section S1). For preparation of the Ab–MNPs, protein A is conjugated to thiolated MNPs through a sulpho-SMCC (sulphosuccinimidyl-4-[*N*-maleimidomethyl]cyclohexane-1-carboxylate) crosslinker. The DR4 antibody is then conjugated to protein A on MNPs in a DR4 antibody/MNP stoichiometric ratio of 1:1 (Fig. 2b and Supplementary Section S1).

For *in vitro* magnetic switching On of apoptosis, Ab–MNPs (1 pM) are applied to DLD-1 colon cancer cells ($1.5 \times 10^4$ cells per well), expressing DR4s (Supplementary Section S2), and the cells are placed in between two NdFeB magnets (Fig. 2c). In the absence of magnetic field, Ab–MNPs are observed as an evenly dispersed weak green fluorescence signal (Fig. 2d(i)) and remain dispersed over time (Supplementary Section S3). However, large aggregated spots exhibiting a strong green fluorescence signal are observed after the application of a magnetic field for 2 h (Fig. 2d(ii) red circles and Supplementary Section S4). Scanning electron microscope (SEM) images consistently show that the initial evenly distributed Ab–MNPs change to densely populated aggregates (Fig. 2e and Supplementary Section S4). Here, the simulated magnetic field is 0.20 T at the centre[28] and the average

[1]Department of Chemistry, Yonsei University, Seoul 120-749, Korea, [2]Graduate Program for Nanomedical Science, Yonsei University, Seoul 120-749, Korea, [3]Department of Internal Medicine, Institute of Gastroenterology, College of Medicine, Yonsei University, Seoul 120-752, Korea, [4]Department of Microbiology, Severance Biomedical Science Institute, Institute for Immunology and Immunological Diseases, College of Medicine, Yonsei University, Seoul 120-752, Korea. †These authors contributed equally to this work. *e-mail: jsshin6203@yuhs.ac; jcheon@yonsei.ac.kr.

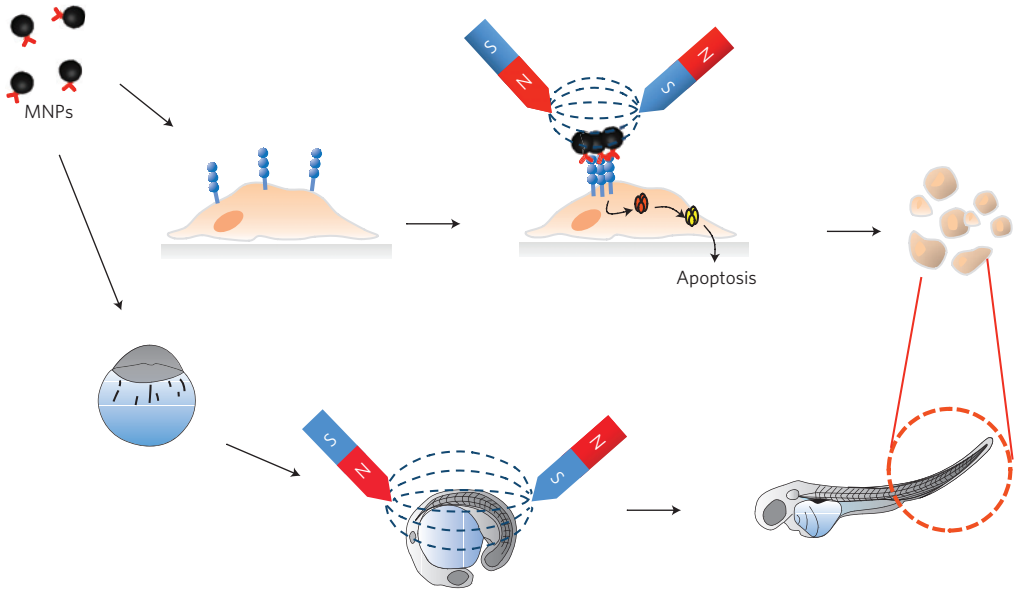


**Figure 1 | A schematic representation of the magnetic switch for apoptosis signalling in *in vitro* cells and in a zebrafish.** MNPs first bind to the death receptors, and subsequent aggregation on the application of a focused magnetic field triggers extrinsic apoptosis signalling. Magnetic switching On of death receptor clustering results in the death of *in vitro* cells and also causes morphological changes in *in vivo* zebrafish.

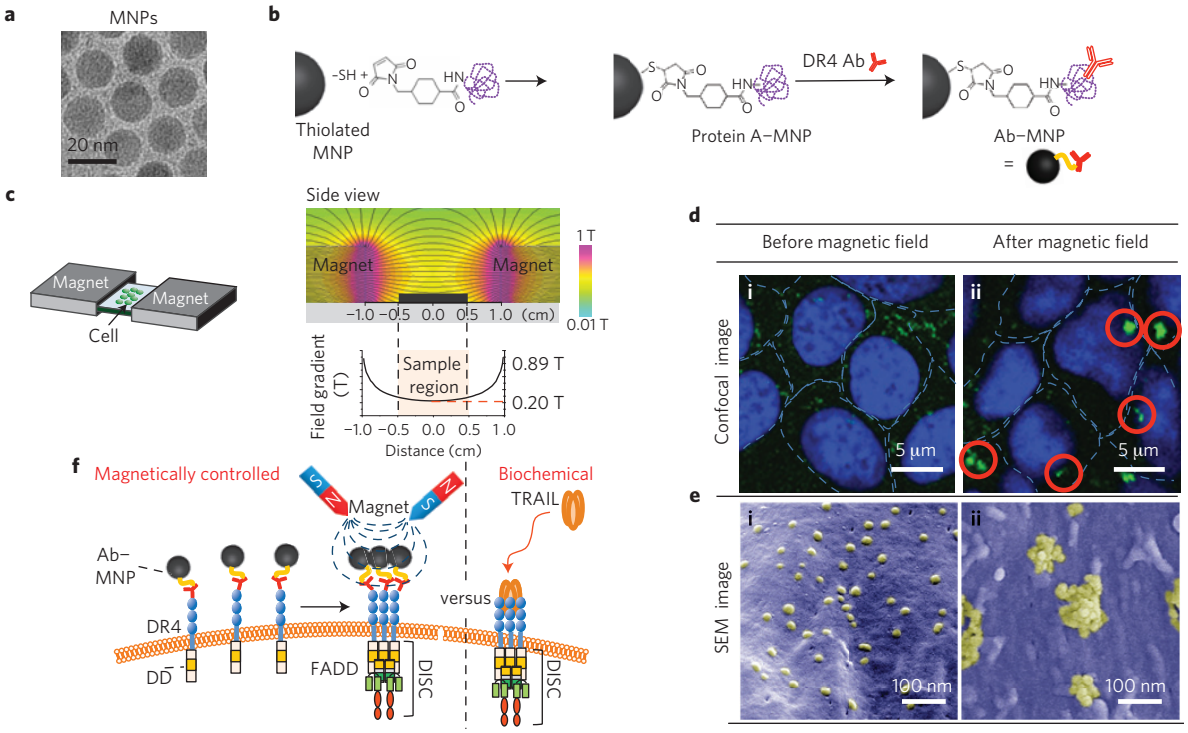


**Figure 2 | Antibody-conjugated MNPs and the magnetic switch set-up for apoptosis signalling. a**, Transmission electron micrograph of 15 nm zinc-doped iron oxide MNPs ($Zn_{0.4}Fe_{2.6}O_4$). **b**, Scheme showing the conjugation of a MNP to the DR4 antibody (DR4 Ab). A thiolated MNP is linked to protein A using sulpho-SMCC (protein A–MNP), and then further conjugated to DR4 Ab (Ab–MNPs). **c**, The magnetic switch set-up for apoptosis signalling. The cell culture plate is placed between two NdFeB magnets and the direction and strength of the magnetic field are indicated as a solid line and colour map, respectively. **d**,**e**, Confocal microscope (**d**) and SEM (**e**) images of Ab–MNP (1 pM)-treated DLD-1 cells ($1.5 \times 10^4$ cells per well) before (i) and after (ii) magnetic field application (2 h). Blue: DAPI (4′,6-diamidino-2-phenylindole)-stained nucleus; green: fluorescein-conjugated Ab–MNPs. The dashed lines are drawn to show the morphology of the cells. The SEM images are false-coloured for clear visibility where Ab–MNPs are shown in yellow. Clustered Ab–MNPs are observed only when a magnetic field is applied, both in the confocal and SEM images. **f**, The magnetic switch for the induction of apoptosis signalling through receptor aggregation, which mimics the biochemical signalling through TRAIL.

distance between the nanoparticles in the sample is 60 nm (as measured by SEM images). The interparticle attraction force is calculated to be about 30 fN, adequate to promote clustering of the Ab–MNPs on the cell membrane[15,29,30] (Supplementary Section S5) without inducing damage to the cell membranes (Supplementary Section S6), whereas that of the gradient force (about 12 zN) is

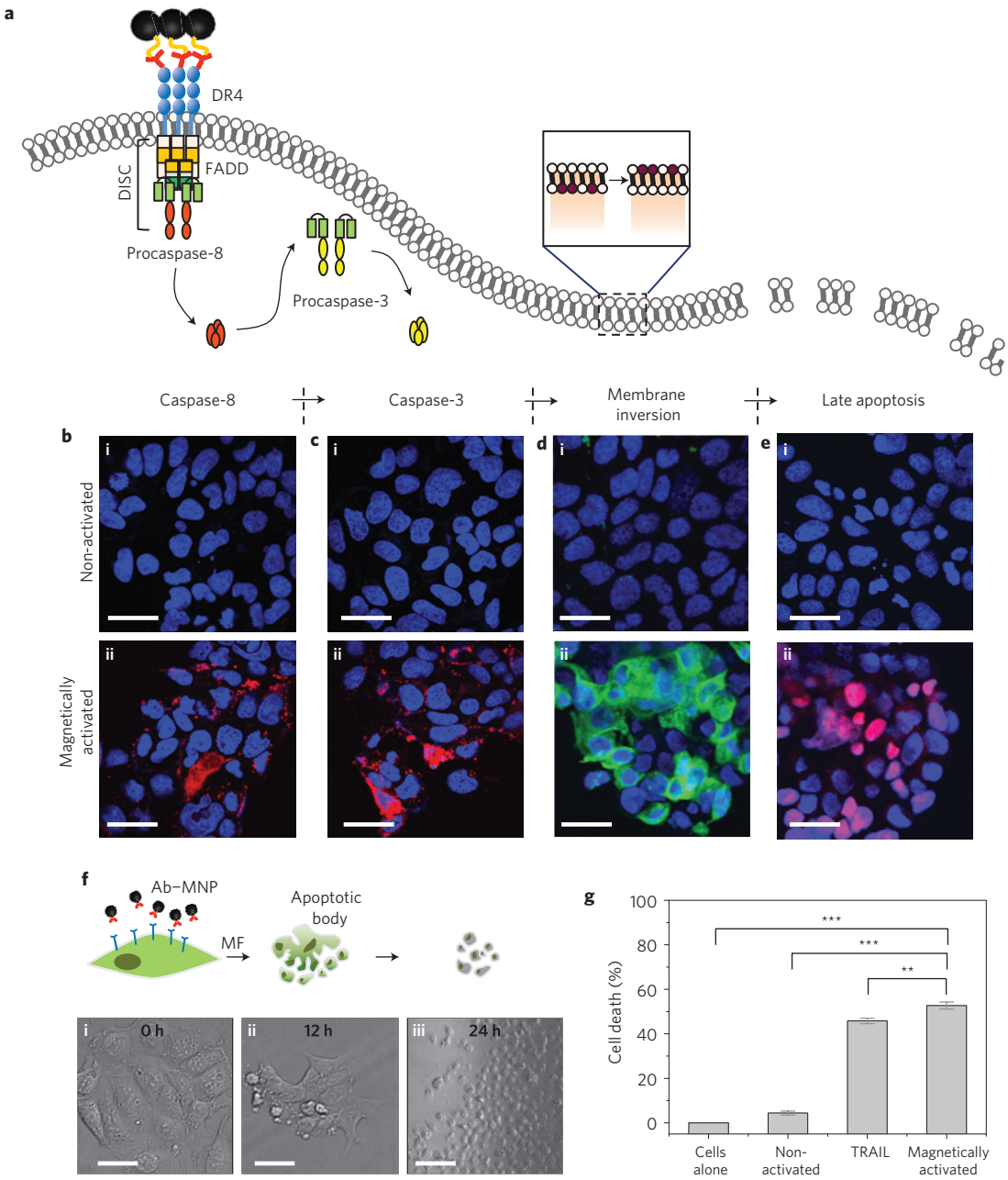


**Figure 3 | *In vitro* apoptosis induction in the DLD-1 colon cancer cell line. a**, Cascade of extrinsic apoptosis signalling pathways. Assembly of DR4s leads to recruitment of DISC, composed of FADD and procaspase-8. Procaspase-8 is cleaved to form active caspase-8 and leads to subsequent caspase-3 activation. **b**,**c**, Confocal microscope images of fluorescently stained active caspase-8 (**b**) and active caspase-3 (**c**) in DLD-1 cells for non-activated (i) and magnetically activated (ii) groups. Active caspase-8 and caspase-3 are immunostained with Alexa-594-labelled secondary antibodies (red) and nuclei are stained with DAPI (blue). **d**,**e**, Confocal micrographs of membrane inversion (**d**) and blebbing at the late apoptosis stage (**e**), stained with FITC–annexin V (green) and propidium iodide (red), respectively. **f**, Differential interference contrast micrographs of DLD-1 cell morphology before (i), 12 h (ii) and 24 h (iii) after magnetic field application. Scale bars, 10 μm. **g**, Cell death measured by CCK-8 assay. Cells treated with Ab–MNPs (1 pM) and magnetic field are compared with the cells alone, Ab–MNPs without magnetic field and TRAIL treatment. Error bars represent standard deviation. ($^{**}P < 0.01$, $^{***}P < 0.001$.)

orders of magnitude weaker and negligible in this set-up where the mid-point of the sample area is 1 cm away from the magnet[15] (Supplementary Section S5). The Ab–MNPs induce clustering of the DR4s in a similar manner to the biochemical ligand, TRAIL, and they have the unique advantage of being magnetically switched On to activate cell signalling remotely and non-invasively in a spatially and temporally controlled fashion (Fig. 2f).

To examine the extrinsic apoptosis signalling process with concurrent assembly of DR4s promoted by using the magnetic switch, biologically important intermediate species of the signalling cascades are monitored. It is known that clustering of DR4s forms the death-inducing signalling complex (DISC) containing the Fas-associated death domain (FADD) and procaspase-8 (refs 20–22). In the DISC, procaspase-8 is cleaved to active caspase-8 (initiator caspase), which leads to further activation of caspase-3 (Fig. 3a). Treatment of Ab–MNPs (1 pM) on DLD-1 cells for 2 h with a 0.20 T magnetic field results in a strong red fluorescence signal arising from the active caspase-8 in the cytoplasm, but no fluorescence is observed in the control group not exposed to a magnetic field (Fig. 3b). Subsequent generation of active caspase-3,

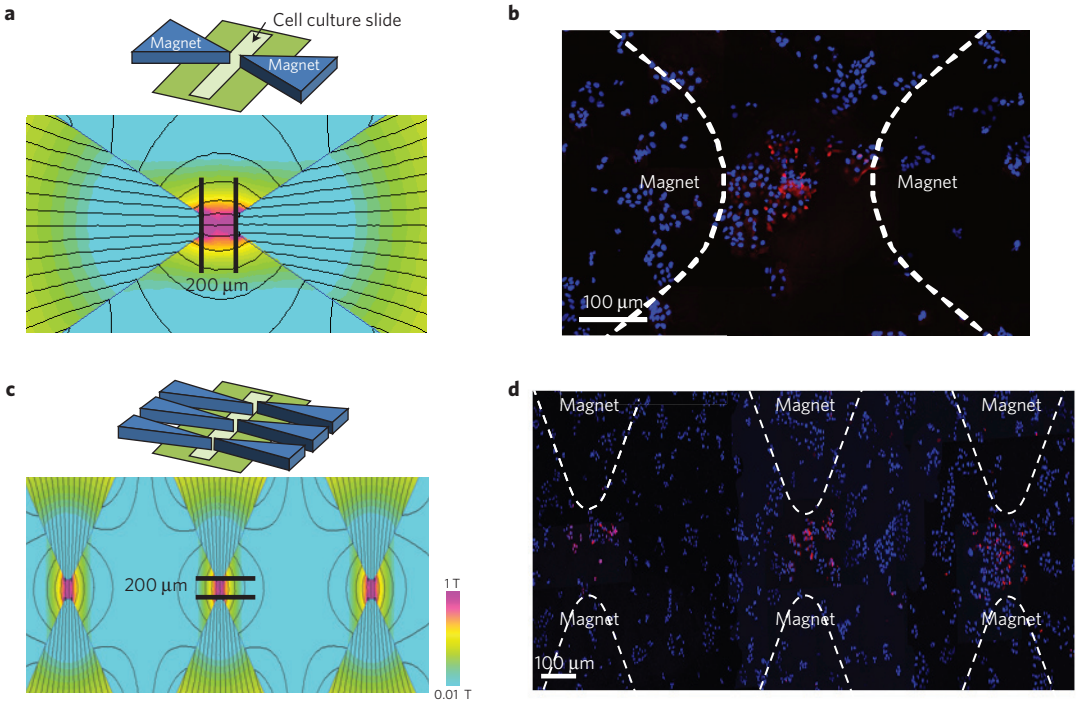


**Figure 4 | Spatial control of apoptosis signalling.** Ab–MNPs (1 pM) are applied to a cell culture slide containing DLD-1 cells with DR4s. **a**,**c**, A single spot (**a**) or three spots (**c**) of magnetic field focused on the cell culture slide. **b**,**d**, Fluorescence micrographs of the active caspase-3 (red) signal merged with DAPI-stained nuclei (blue). Each image is created by stitching 50–120 fluorescence images pictured by ×200 magnification confocal microscope.

indicated by a red fluorescence signal, is observed only for magnetically activated DLD-1 cells (Fig. 3c). Apoptosis signalling through caspase activation does not occur when each component of the magnetic switch, such as magnetic field, antibody or MNP, is applied alone (Supplementary Section S7). It is known that clustering of surface receptor DR4s by a biochemical ligand, such as TRAIL, initiates apoptosis signalling and then facilitates their endocytosis into the cytoplasm[24,25]. Similarly, for MNPs bound to DR4s, we observe that about 30% of the MNPs are endocytosed and about 70% are still on the membrane after 2 h of magnetic field application (Supplementary Section S8).

Caspase-3, known to be an effector caspase and death signal, is strongly amplified in cooperation with other members of the caspase family[31]. Entry of the cell into the demolition phase is associated with membrane inversion and blebbing at the late apoptosis stage as major phenomena[17–19]. The occurrence of these changes is confirmed by using FITC (fluorescein isothiocyanate)–annexin V and propidium iodide staining, respectively. The observation of a bright fluorescence signal, which is not observed in magnetically non-activated cells, is a clear indicator of this apoptotic outcome (Fig. 3d,e). Moreover, temporal morphological changes of the cells are also monitored during the magnetically activated apoptotic process. In comparison with that of normal cells, $1.5 \times 10^4$ cells treated with Ab–MNPs (1 pM; Fig. 3f(i)) gradually shrink and fragment after 12 and 24 h application of the magnetic field (Fig. 3f(ii, iii)). Quantitative analysis of apoptosis, using a cell counting kit-8 (CCK-8) assay, shows that about 52% of the cells treated with Ab–MNPs are dead after magnetic activation, whereas the cells in the non-activated group remain viable (Fig. 3g). This level of efficacy is slightly higher than that of TRAIL, the biochemical ligand previously employed as an extrinsic apoptosis signalling agent and potential cancer drug[20–26], which induces cell death in about 45% of the cells treated under the same conditions. We also observe that the cell death rate is dependent on the concentration of Ab–MNPs (Supplementary Section S9). Apoptosis signalling, induced in this manner by the magnetic switch, requires a minimum magnetic field of about 0.03 T (Supplementary Section S10). The degree of apoptosis signalling responds proportionally to the applied magnetic field strength (Supplementary Section S10) and the magnetic field application time (Supplementary Section S11), but is not affected by the direction of the magnetic field (Supplementary Section S12).

In contrast to biochemical ligands that typically induce systemic stimulation of cell signalling in the whole body[23–26], the magnetic switch system has the merit of spatial controllability using the application of an attenuated magnetic field to a selected area. To demonstrate local activation of apoptosis signalling, a 0.64 T magnetic field is focused to a micrometre-size area of a cell culture slide containing DLD-1 cells by using the magnetic set-up shown in Fig. 4a. On application of the magnetic field for 4 h, activation of caspase-3, seen in the form of an immunostained red fluorescence signal, is observed to occur exclusively in the area of about 200 μm × 100 μm between the magnets (Fig. 4b). Similarly, active caspase-3 is consistently observed in an array comprising magnetic focusing on three local spots (Fig. 4c,d), which testifies to the spatial controllability of the magnetic switching technique.

Although this magnetic switching strategy for apoptosis signalling is effective at the *in vitro* level, its further extension to *in vivo* activation is both significant and challenging because of the complexity of live biological systems. We choose zebrafish as an *in vivo* model not only because of the benefits associated with optical imaging and convenient screening[32–34], but also because of the genetic closeness of the zebrafish ovarian TNF receptor (OTR) to the human DR4 for apoptosis signalling[35,36]. Zebrafish OTRs are targeted and magnetically manipulated by using zebrafish OTR antibody conjugated to MNPs (zAb–MNPs). First, fluorescein-labelled zAb–MNPs (2.5 ng per embryo) are micro-injected into the yolk of the zebrafish embryo at the one-cell stage of growth. After 24 h, pronase is used to hatch the zebrafish embryos, which are then divided into two groups including those that will and will not be magnetically activated. For the magnetically activated group, a magnetic field with a strength of

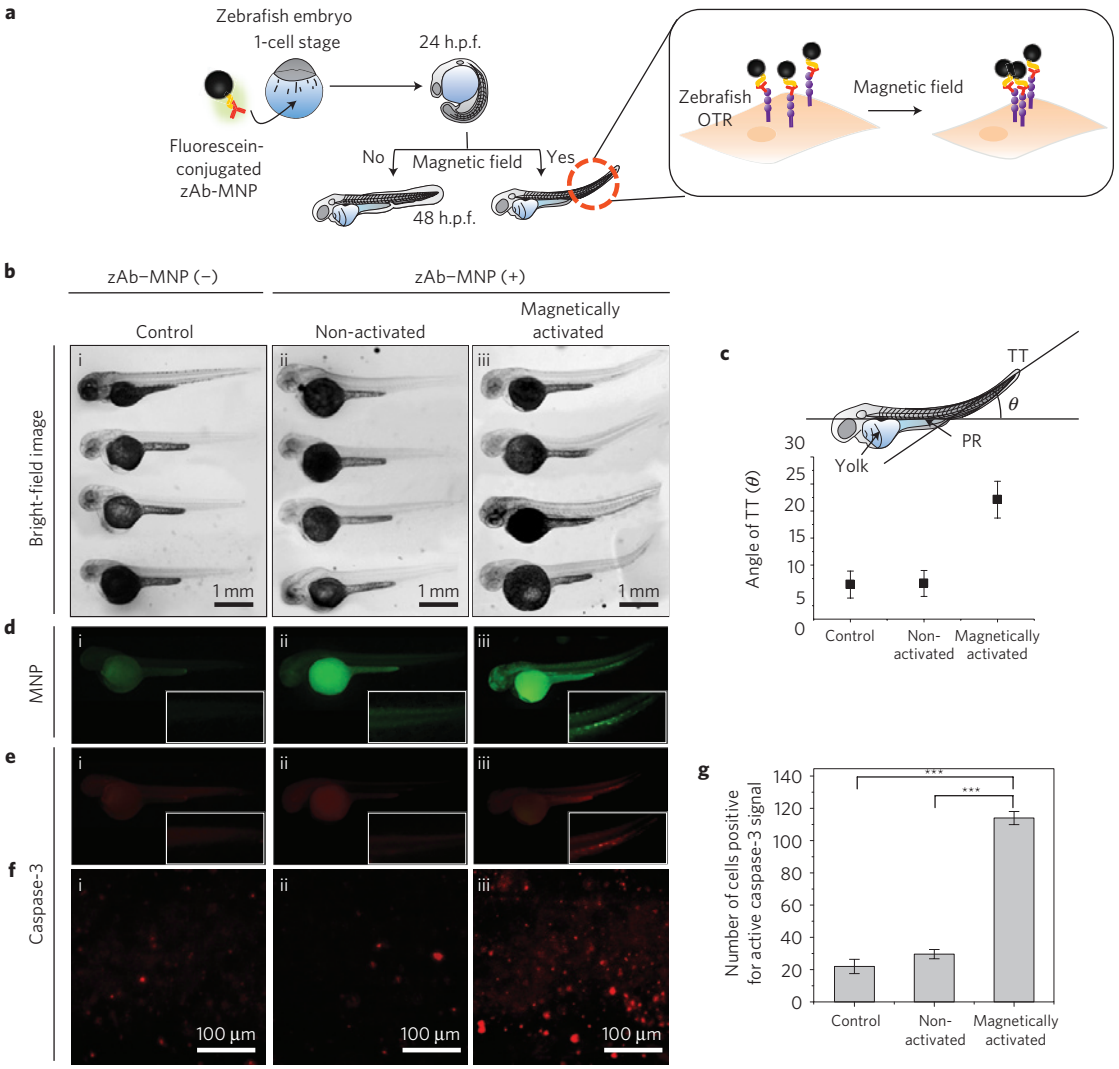


**Figure 5 | *In vivo* magnetic apoptosis signalling for zebrafish. a**, The apoptosis experimental scheme of zebrafish. Fluorescein-labelled zAb–MNPs (2.5 ng embryo$^{-1}$) are micro-injected into yolk of embryo at one-cell stage to label extrinsic apoptosis receptor (OTR). At 24 h post-fertilization (h.p.f.), the magnetic field is applied to zebrafish. **b**, Bright-field microscope images of three different groups of zebrafish, control (i), non-activated (ii) and magnetically activated (iii). The magnetically activated group of zebrafish shows morphological alterations in the tail region compared with other groups. **c**, Quantitative analysis on tail bending by measuring the angle between the line on the pronephros (PR) and the line of tail tip (TT) for each group. **d**–**f**, Fluorescence images of zebrafish in which zAb–MNPs are green and active caspase-3 is immunostained as red. Green and red fluorescence are only observed in the tail region of the magnetically activated group (**d**(iii),**e**(iii)). Insets in **d** and **e** are magnified images of tail region. **f**, Magnified fluorescence micrographs of active caspase-3 in zebrafish tail region. **g**, A graph of caspase-3 activity measured by using fluorescence intensity of zebrafish. Error bars are standard deviation. (***$P < 0.001$).

0.50 T is applied to a zebrafish chamber for 24 h (Fig. 5a). After application of the magnetic field, characteristic features associated with apoptosis, such as morphological deformation of embryos and caspase-3 activation[35,36], are examined at the 48 h post-fertilization (h.p.f.) stage. Inspection of bright-field microscope images shows that both the control and non-activated groups exhibit normal ontogenic zebrafish embryo development (Fig. 5b(i,ii)). In contrast, morphological alterations in the tail region are clearly observed in images of the magnetically activated group (Fig. 5b(iii)). This morphological change is visualized by determining the angle of tail tip bending. For this purpose, a straight line is drawn along the pronephros and the angles between this line and tail tip line are measured in three different groups, as shown in Fig. 5c. The magnetically activated group shows an approximately 3.5-fold larger angle (about 22°) than that of the control and non-activated groups (about 6°). This morphological change is proposed to be a consequence of apoptosis signalling[35]. Besides, zebrafish embryos without zAb–MNPs injection are not affected by magnetic field application alone (Supplementary Section S7).

To gain further evidence for the occurrence of apoptosis, the location of zAb–MNPs and the apoptosis signalling products are examined using an optical method. zAb–MNPs are fluorescently labelled and the strong green fluorescence signal is observed in the yolk for both the magnetically activated and non-activated groups owing to residual zAb–MNPs after the injection. Interestingly, clumps of strong green fluorescence signal are seen in zebrafish tail regions that are magnetically activated, whereas this region of non-activated zebrafish shows only a dispersed and weak green fluorescence signal (Fig. 5d(ii,iii)). These observations are caused by the combination of higher OTR expression in the tail region of zebrafish in a manner that is consistent with previous observations[35,36], and subsequent magnetic clustering of the OTRs.

The activation of caspase-3 at the tail region is confirmed by using immunostaining. Both the control and non-activated

groups of zebrafish embryos show no apparent signals associated with active caspase-3 (Fig. 5e(i,ii)). In contrast, strong red spots associated with active caspase-3 are clearly observed in the tail region for the magnetically activated group (Fig. 5e(iii),f(iii)), which match closely with the region of green fluorescence signal of clustered zAb–MNPs. Note, the faint red signals seen for the control and non-activated groups in this immunostaining process are due to the naturally occurring mild apoptosis process of zebrafish (Fig. 5f(i,ii)). The results of quantitative measurements of active caspase-3 show that the magnetically activated group has an approximately 6-fold higher fluorescence intensity level than those of the control and non-activated groups (Fig. 5g). It has been documented that a bent tail is regarded as one of the most representative traits of apoptosis[35,36]. Consistent with this, the highly localized presence of OTR receptors, clustered MNPs and activated caspase-3 in the lower part of the tail stem is likely to cause the tail to bend up through localized apoptotic cell death in the tail. The combined results demonstrate that the magnetic switch can be effectively applied to *in vivo* live vertebrates.

In the study described above, we have demonstrated that apoptosis signalling can be turned On *in vitro* and in a zebrafish *in vivo* model by using a magnetic switch. Our magnetic switch may be broadly applicable to any type of surface membrane receptors that exhibit cellular functions on clustering. With apoptosis being one of the main cancer research targets, the development of an extrinsic apoptosis agonist that can avoid p53 mutation-induced drug resistance is important and here our magnetic switch can serve as a selective inducer[19,27]. Likewise, the applications can be extended to other clinically useful membrane receptors, such as the vascular endothelial growth factor receptor for regenerative medicine[37] and the Toll-like receptor for immune potentiation[38]. Although at an early stage of development, the spatially and temporally controlled magnetic switch system has the potential to be a useful tool for the activation of various cell signals at the target region.

Received 20 March 2012; accepted 23 August 2012; published online 7 October 2012

## References


1. Hoffman, B. D., Grashoff, C. & Schwartz, M. A. Dynamic molecular processes mediate cellular mechanotransduction. *Nature* **475,** 316–323 (2011).
2. Gorostiza, P. & Isacoff, E. Y. Optical switches for remote and noninvasive control of cell signaling. *Science* **322,** 395–399 (2008).
3. Lee, S. E., Liu, G. L., Kim, F. & Lee, L. P. Remote optical switch for localized and selective control of gene interference. *Nano Lett.* **9,** 562–570 (2009).
4. Chung, I. *et al.* Spatial control of EGF receptor activation by reversible dimerization on living cells. *Nature* **464,** 783–787 (2010).
5. Jang, J-t. *et al.* Critical enhancements of MRI contrast and hyperthermic effects by dopant-controlled magnetic nanoparticles. *Angew. Chem. Int. Ed.* **48,** 1234–1238 (2009).
6. Jordan, J. D., Landau, E. M. & Iyengar, R. Signaling networks: The origins of cellular multitasking. *Cell* **103,** 193–200 (2000).
7. Pankhurst, Q. A., Connolly, J., Jones, S. K. & Dobson, J. Application of magnetic nanoparticles in biomedicine. *J. Phys. D* **36,** R167–R181 (2003).
8. Gupta, A. K. & Gupta, M. Synthesis and surface engineering of iron oxide nanoparticles for biomedical applications. *Biomaterials* **26,** 3995–4021 (2005).
9. Huang, H., Delikanli, S., Zeng, H., Ferkey, D. M. & Pralle, A. Remote control of ion channels and neurons through magnetic-field heating of nanoparticles. *Nature Nanotech.* **5,** 602–606 (2010).
10. Creixell, M. *et al.* EGFR-targeted magnetic nanoparticle heaters kill cancer cells without a perceptible temperature rise. *ACS Nano* **5,** 7124–7129 (2011).
11. Wang, N., Butler, J. P. & Ingber, D. E. Mechanotransduction across the cell surface and through the cytoskeleton. *Science* **260,** 1124–1127 (1993).
12. Kanczler, J. M. *et al.* Controlled differentiation of human bone marrow stromal cells using magnetic nanoparticle technology. *Tissue Eng.* **16,** 3241–3250 (2010).
13. Hughes, S., Haj, A. J. E. & Dobson, J. Magnetic micro- and nanoparticle mediated activation of mechanosensitive ion channels. *Med. Eng. Phys.* **27,** 754–762 (2005).
14. Dobson, J. Remote control of cellular behavior with magnetic nanoparticles. *Nature Nanotech.* **3,** 139–143 (2008).
15. Mannix, R. J. *et al.* Nanomagnetic actuation of receptor-mediated signal transduction. *Nature Nanotech.* **3,** 36–40 (2008).
16. Lee, J-H. *et al.* Artificial control of cell signaling and growth by magnetic nanoparticles. *Angew. Chem. Int. Ed.* **49,** 5698–5702 (2010).
17. Danial, N. N. & Korsmeyer, S. J. Cell death: Critical control points. *Cell* **116,** 205–219 (2004).
18. Williams, G. T. Programmed cell death: Apoptosis and oncogenesis. *Cell* **65,** 1097–1098 (1991).
19. Storey, S. Targeting apoptosis: Selected anticancer strategies. *Nature Rev.* **7,** 971–972 (2008).
20. Fulda, S. & Debatin, K-M. Extrinsic versus intrinsic apoptosis pathways in anticancer chemotherapy. *Oncogene* **25,** 4798–4811 (2006).
21. Ashkenazi, A. Targeting death and decoy receptors of the tumour-necrosis factor superfamily. *Nature Rev. Cancer* **2,** 420–430 (2002).
22. Sayers, T. J. Targeting the extrinsic apoptosis signaling pathway for cancer therapy. *Cancer Immunol. Immunother.* **60,** 1173–1180 (2011).
23. Mahalingam, D., Szegezdi, E., Keane, M., Jong, S. de & Samali, A. TRAIL receptor signaling and modulation: Are we on the right TRAIL? *Cancer Treat. Rev.* **35,** 280–288 (2009).
24. Vondálová Blanárová, O. *et al.* Cisplatin and a potent platinum(IV) complex-mediated enhancement of TRAIL-induced cancer cells killing is associated with modulation of upstream events in the extrinsic apoptotic pathway. *Carcinogenesis* **32,** 42–51 (2011).
25. Schneider-Brachert, W. *et al.* Compartmentalization of TNF receptor 1 signaling: Internalized TNF receptosomes as death signaling vesicles. *Immunity* **21,** 415–428 (2004).
26. Kelley, S. K. & Ashkenazi, A. Targeting death receptors in cancer with Apo2L/TRAIL. *Curr. Opin. Pharmacol.* **4,** 333–339 (2004).
27. Ashkenazi, A. & Herbst, R. S. To kill a tumor cell: The potential of proapoptotic receptor agonists. *J. Clin. Invest.* **118,** 1979–1990 (2008).
28. Meeker, D. C. Finite element method magnetics. http://www.femm.info (accessed Feb 9, 2011).
29. Türkcan, S. *et al.* Observing the confinement potential of bacterial pore-forming toxin receptors inside rafts with nonblinking $Eu^{3+}$-doped oxide nanoparticles. *Biophys. J.* **102,** 2299–2308 (2012).
30. Pralle, A., Keller, P., Florin, E-L., Simons, K. & Hörber, J. K. H. Sphingolipid-cholesterol rafts diffuse as small entities in the plasma membrane of mammalian cells. *J. Cell Biol.* **148,** 997–1007 (2000).
31. Porter, A. G. & Jänicke, R. U. Emerging roles of caspase-3 in apoptosis. *Cell Death Differ.* **6,** 99–104 (1999).
32. Pyati, U. J., Look, A. T. & Hammershmidt, M. Zebrafish as a powerful vertebrate model system for *in vivo* studies of cell death. *Semin. Cancer Biol.* **17,** 154–165 (2007).
33. Eimon, P. M. & Ashkenazi, A. The zebrafish as a model organism for the study of apoptosis. *Apoptosis* **15,** 331–349 (2010).
34. Yamashita, M. Apoptosis in zebrafish development. *Comp. Biochem. Phys. B* **136,** 731–742 (2003).
35. Eimon, P. M. *et al.* Delineation of the cell-extrinsic apoptosis pathway in the zebrafish. *Cell Death Differ.* **13,** 1619–1630 (2006).
36. Bobe, J. & Goetz, F. W. Molecular cloning and expression of a TNF receptor and two TNF ligands in the fish ovary. *Comp. Biochem. Phys. B* **129,** 475–481 (2001).
37. Matsuda, H. The current trends and future prospects of regenerative medicine in cardiovascular diseases. *Asian Cardiovasc. Thorac. Ann.* **13,** 101–102 (2005).
38. Oblak, A. & Jerala, R. Toll-like receptor 4 activation in cancer progression and therapy. *Clin. Dev. Immunol.* **475,** 1–12 (2011).


## Acknowledgements

This work was financially supported by grants from the Creative Research Initiative (2010-0018286), WCU Program (R32-10217), National Research Foundation of Korea (2011-0017611) and the second stage BK21 for Chemistry and Medical Sciences of Yonsei University. S.W.P. was supported by the National Research Foundation, Mid-career Researcher Program (72011-0043). M.H.C. was supported by a Hi Seoul Science/Humanities Fellowship from the Seoul Scholarship Foundation.

## Author contributions

J.C. and J-S.S. conceived and designed the experiments. M.H.C., E.J.L., M.S. and J-w.K. performed the experiments. S.W.P. provided advice on the *in vivo* zebrafish experiments. M.H.C., E.J.L., J-H.L., D.Y., J-S.S. and J.C. wrote the manuscript.

## Additional information

Supplementary information is available in the online version of the paper. Reprints and permissions information is available online at www.nature.com/reprints. Correspondence and requests for materials should be addressed to J-S.S. or J.C.

## Competing financial interests

The authors declare no competing financial interests.